

Closed-loop control of a long-range micropositioner using integrated photodiode sensors

Mustafa Ilker Beyaz*, Matthew McCarthy, Nima Ghalichechian, Reza Ghodssi*

MEMS Sensors and Actuators Laboratory, Department of Electrical and Computer Engineering, Institute for Systems Research, University of Maryland, College Park, MD, USA

ARTICLE INFO

Article history:

Received 16 October 2008

Received in revised form 11 February 2009

Accepted 11 February 2009

Available online 28 February 2009

Keywords:

Micropositioners
Closed-loop control
Feedback sensors
Photodiodes
MEMS

ABSTRACT

Closed-loop control of an electrostatically actuated micropositioner using integrated feedback sensors is reported. A photodiode-based position sensing mechanism has been incorporated into a variable-capacitance micromotor supported on microball bearings with a range of 4 mm and a resolution of 120 μm . Accurate and reliable positioning has been demonstrated using a proportional control law and the effect of the proportionality constant has been investigated for various stepping distances and actuation voltages. A minimum settling time of 0.1 s was achieved for a 1 mm step at 150 V. Closed-loop excitation has enabled sustained synchronous motion and a maximum speed of 20.4 mm/s. This is a noted improvement compared to open-loop excitation, which exhibits erratic motion and a maximum speed of 7.2 mm/s. Using feedback control, two critical functions for robust positioning have been demonstrated; the micropositioner can establish a necessary frame of reference and autonomously respond to arbitrary disturbances. The closed-loop position control system presented in this work illustrates the feasibility and functionality of smart microsystems using integrated feedback sensors.

© 2009 Elsevier B.V. All rights reserved.

1. Introduction

Micropositioners capable of accurate and reliable operation over long actuation ranges are required for a variety of next-generation applications. The development of such micropositioners is essential for the realization of high-performance optical switching, data storage, and surface scanning components within compact low-cost distributed microsystems. The current work focuses on the development of an integrated feedback control system for dynamic micropositioning of a variable-capacitance micromotor supported on microball bearings. Closed-loop position control, along with reliable millimeter-range microball bearings and a simple electrostatic actuation principle, are used to demonstrate the viability of smart microsystems using integrated feedback sensing.

Micro-actuators and positioners have been demonstrated with a variety of actuation mechanisms including electrostatic, thermal, magnetic, and piezoelectric. Patrascu and Stramigioli [1] and Lee et al. [2] have reported micropositioners using electrostatic actuation in stepper and comb drive configurations, respectively, with displacement ranges of less than 200 μm . Additionally, a cantilever-based optical switch using electrostatic actuation to bend waveguide structures has been demonstrated [3]. The tethered nature of these devices couples the actuation forces and

displacement distances, limiting their operation to specific deflections and precluding their use in long-range applications. Devices using a similar tethered design and thermal actuation have been reported for ranges of up to a few hundred microns [4,5]. In addition to range limitations, these devices require large temperatures and temperature gradients to provide actuation. Magnetic and piezoelectric actuation mechanisms have also been used to develop microfabricated positioners with ranges of up to 12 μm [6,7]. While an inchworm micropositioner capable of moving up to several millimeters has been developed by Cusin et al. [8], the actuation speed ($\sim 300 \mu\text{m/s}$) is likely too slow for most applications.

Robust and repeatable actuation requires integrated feedback control, and accordingly, has been investigated for microfabricated positioning systems. Chu and Gianchandani [9] developed a two-dimensional electro-thermally actuated micropositioner using capacitive position sensors for feedback control. They were able to achieve high-resolution positioning over a 19 μm range. Similarly, an electrostatic micropositioner with capacitive sensing and a positioning range of 2.8 μm was demonstrated by Horsley et al. [10]. Continued work in the field of closed-loop control for MEMS-fabricated actuators is required for the realization of high-performance microsystems capable of accurate and long-range positioning.

Previous work by our group has demonstrated variable-capacitance micromotors supported on linear microball bearings [11,12], including characterization of the drive mechanism using benzocyclobutene (BCB)-embedded electrodes [13–16] as well as

* Corresponding authors.

E-mail addresses: beyaz@umd.edu (M.I. Beyaz), ghodssi@umd.edu (R. Ghodssi).

the microball support mechanism [16–19] and photodiode feedback sensing [20–22]. Electrostatics and linear microball bearings have been shown to be stable and robust actuation and support mechanisms created through simple fabrication processes. The range of these devices is limited by the length of the microball housings, while the positioning resolution is dictated by the variable-capacitance electrode spacing. Using such a design, the actuation force and translation distance have been decoupled. This allows for a continuous in-plane force to be applied over the entire range of displacement, making these devices highly desirable for long-range applications. This design, however, is susceptible to random disturbances and variations in microball rolling friction leading to erratic behavior. Accordingly, this work focuses on the development of integrated photodiode-based position sensors and a proportional control law to drive such devices under closed-loop excitation.

2. Device components

The micropositioner presented here is comprised of a linear electrostatic micromotor with integrated photodiode sensors for feedback control. The design, fabrication, and characterization of the micromotor have been previously reported [12], demonstrating millimeter-range actuation using microball bearings as a support mechanism. In the current work, photodiode-based position sensors have been implemented, providing feedback signals for closed-loop control.

2.1. Linear micromotor

A schematic representation of the variable-capacitance micromotor and its actuation principle is shown in Fig. 1 [12]. The micromotor consists of a silicon slider supported on microball bearings ($\varnothing = 285 \mu\text{m}$) over an array of stator electrodes embedded in low- k benzocyclobutene (Fig. 1a). Electrical forces align the salient poles etched on the slider with the excited electrodes on the stator. Continuous motion is created by sequential excitation of the electrodes in a three-phase configuration. To prevent charge build up on the slider, each phase is applied in positive–negative pairs, resulting in six discrete excitation signals (Fig. 1b).

In the previously reported devices, loss of synchronization was observed using open-loop excitation; this is primarily attributed to the nature of microscale rolling friction. As the slider translates, the resistance to rolling fluctuates due to differences between sliding and rolling friction as well as variations in the surface roughness, sidewall contact, and slide-to-roll ratio. As a result, the slider arbitrarily loses and regains synchronization with the electrical excitation, and random variations in the trajectory are observed.

2.2. Photodiode-based position sensing

The erratic nature of the micromotor under open-loop excitation precludes its use as a reliable actuation mechanism for positioning applications. Feedback control is therefore necessary for accurate positioning and repeatable operation. Accordingly, photodiodes have been integrated with the linear electrostatic micromotor to provide feedback signals for closed-loop excitation. Fig. 2 shows exploded and assembled views of the current device, illustrating the position sensing mechanism developed for this work.

The existing micromotor design [12] has been modified to include metal–semiconductor–metal photodiodes on the stator and etched through-holes on the slider. The location and geometry of the electrodes, poles, photodiodes and through-holes are such that photodiode–hole and electrode–pole pairs are aligned simultaneously. Exposing light from the topside, the position is tracked by

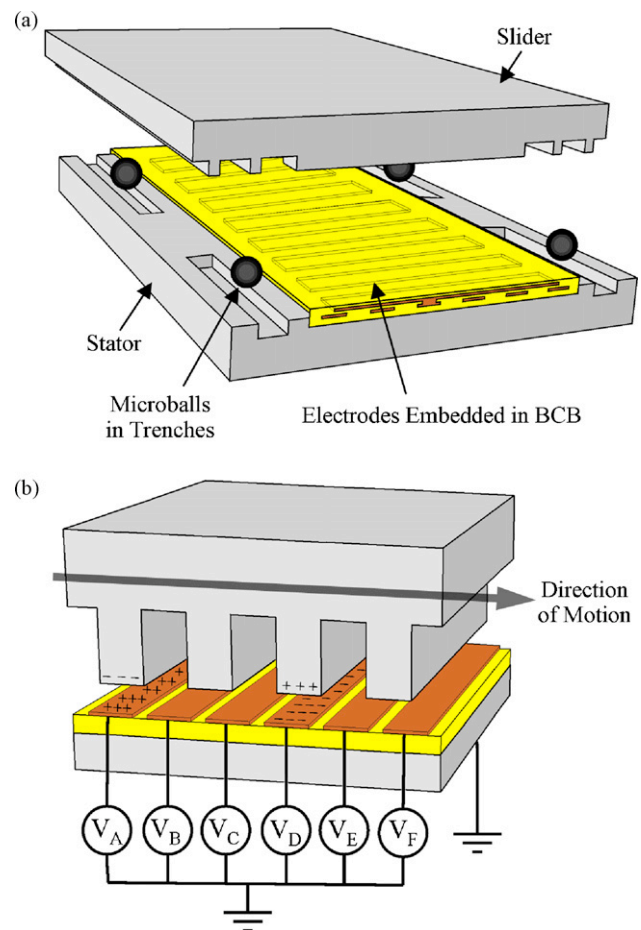


Fig. 1. Schematic representations of (a) the micromotor design showing the slider, stator, microballs ($\varnothing = 285 \mu\text{m}$), and electrodes and (b) the variable-capacitance actuation mechanism with six distinct excitation signals [12].

monitoring photodiode current as the slider translates, while a high-speed camera is used to independently track position (Fig. 2b).

Using an op-amp transimpedance amplifier with negative gain, the photodiode output current is converted to a voltage signal. Fig. 3 shows the response of a single photodiode as the slider is actuated at 75 mm/s using external means. Through-hole to photodiode alignment and misalignment corresponds to local minimums and maximums in voltage, respectively. These results show low-noise linear variations in photodiode output as the slider translates with

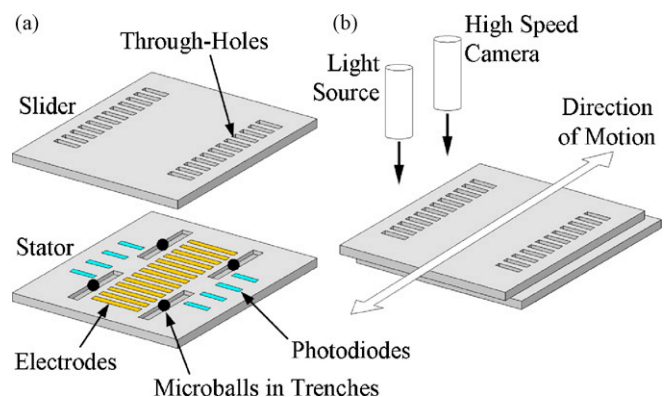


Fig. 2. Schematic representations of (a) an exploded micropositioner showing through-holes and photodiode structures and (b) the assembled device's operating principle showing the light source and high-speed camera for experimental characterization.

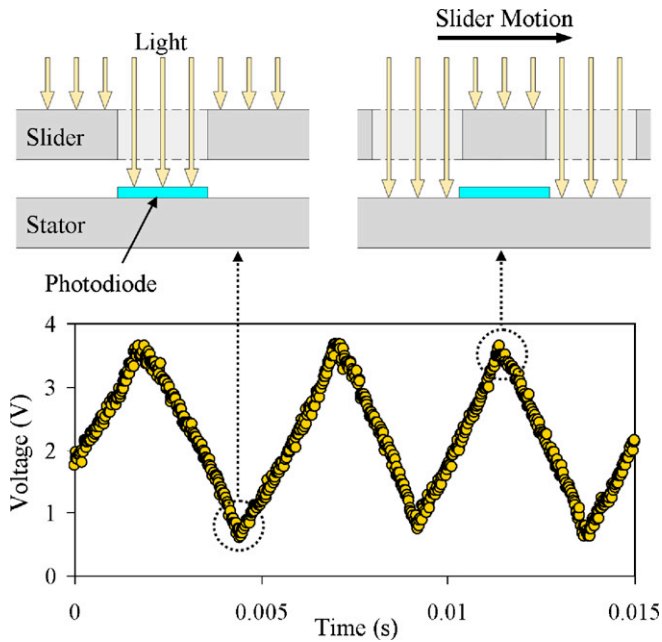


Fig. 3. Photodiode position sensor response showing the local minima and maxima associated with alignment and misalignment of the through-holes and photodiode.

a signal to noise ratio of 23.5 dB and a position sensing resolution of less than 10 μm .

3. Fabrication

The micropositioner fabrication process is shown in Fig. 4. A 300 nm thick aluminum layer is sputtered on a n-type silicon wafer, forming a Schottky contact. Interdigitated metal–semiconductor–metal photodiodes are patterned and etched with finger widths of 4 μm , spacings of 7 μm , and an overall footprint of 180 $\mu\text{m} \times 1 \text{ mm}$ (Fig. 4a). The photodiodes are then protected with photoresist, while electrodes embedded in BCB are fabricated using a previously developed process [11–15] (Fig. 4b). The stator fabrication is completed by deep-etching the microball trenches (Fig. 4c). The slider is created on a separate wafer by etching poles, through-holes, and microball trenches using a two-step DRIE process (Fig. 4d and e). Finally, the sliders are diced and the device is assembled with stainless steel microballs ($\varnothing = 285 \mu\text{m}$) defining a 10 μm gap between the stator electrodes and slider poles (Fig. 4f). Fig. 5 shows photographs of the fabricated device and pertinent structures. The electrodes are 180 μm wide with a 60 μm spacing (Fig. 5a) while the poles are 180 μm wide with a 180 μm spacing (Fig. 5c), resulting in a 3:2 electrode-to-pole ratio. The total range and the minimum stepping distance of the micropositioner are 4 mm and 120 μm , respectively.

4. Testing and results

Fig. 6 shows an assembled device where six probes provide electrical excitation to the stator and a white light source is used to illuminate the photodiodes. Three photodiode currents are converted into voltages through transimpedance amplifiers and used as feedback signals for closed-loop control. A high-speed camera (Motion Pro H-3) and motion tracking software (ProAnalyst) are used to independently characterize the micropositioner response.

The micropositioner resolution, as dictated by the electrode–pole geometry, is 120 μm . The device can therefore move in multiples of this minimum stepping distance up to a maximum range of 4 mm defined by the maximum extent of the

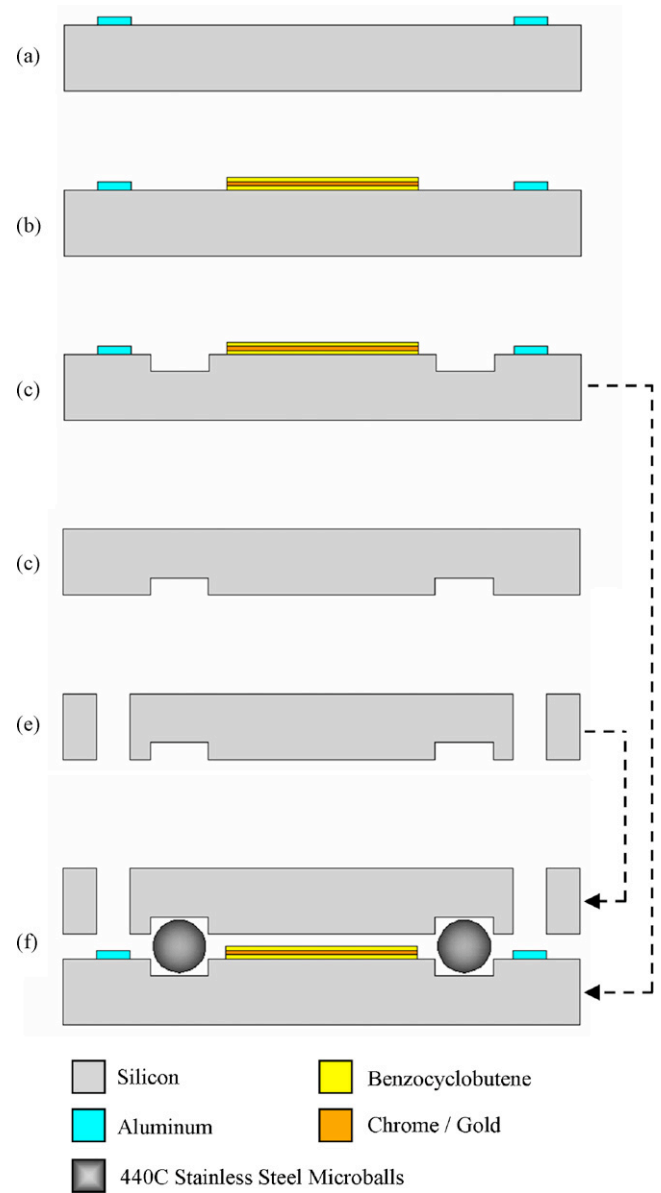


Fig. 4. Micropositioner fabrication process flow showing: (a) interdigitated aluminum photodiodes sputtered and patterned, (b) chrome/gold electrodes embedded in BCB, (c and d) deep-etched ball housings on the stator and slider, (e) deep-etched through-holes, and (f) the stator and slider assembled using 285 μm diameter stainless steel microballs.

bearing mechanism. Fig. 7 shows the slider trajectory without using a closed-loop control scheme. By sequentially exciting each phase, the slider is stepped forward and backward at the minimum stepping distance. The discrete nature of the electrical excitation results in local oscillations around each new equilibrium position with a natural frequency and an average damping ratio of 20 Hz and 0.025, respectively. These oscillations limit the maximum achievable speed and often lead to a loss of synchronization between the excitation signal and motion [20–22]. Accordingly, a closed-loop control system has been implemented to improve speed and reliability by offsetting the effects of electrostatic spring forces and microscale rolling friction. In addition, closed-loop excitation allows for accurate long-distance positioning without the need for stable alignment at each electrode–pole pair.

Initially, a control system with a proportional-integral-derivative (PID) control law was designed and implemented.

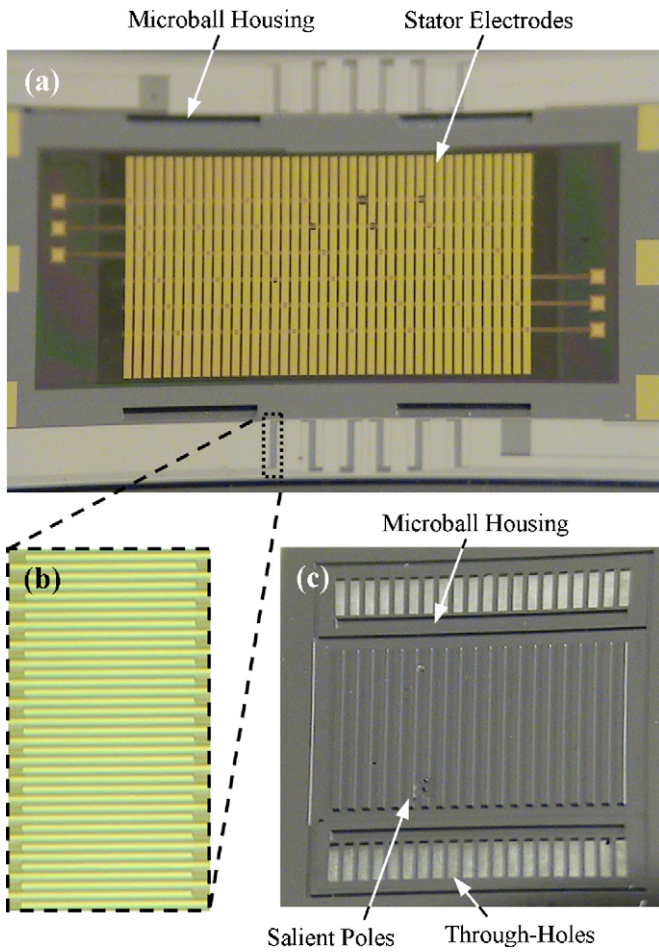


Fig. 5. Photographs of (a) the top view of the fabricated stator showing electrodes, microball trenches, and (b) interdigitated photodiode structures as well as (c) the bottom side of the slider showing poles, through-holes, and microball trenches.

However, the noise introduced by the light source at the sensor signal frequency prevented the derivative and integral terms from functioning properly. Accordingly, a proportional control scheme is used for closed-loop excitation (Fig. 8). The following equation

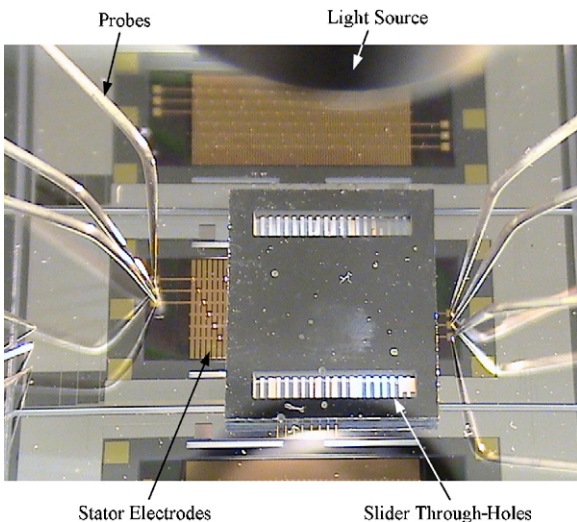


Fig. 6. Photograph of an assembled device being tested showing the stator electrodes, slider through-holes, light source, and probes for excitation.

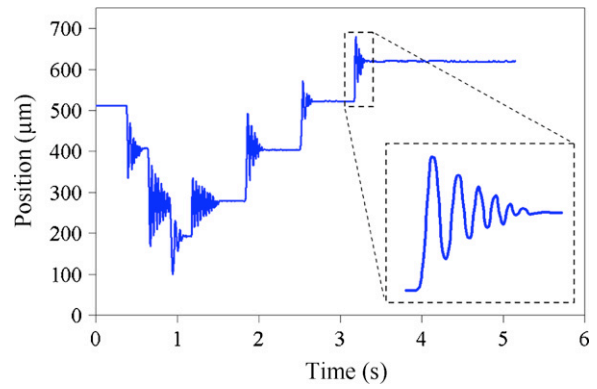


Fig. 7. Slider stepping motion without closed-loop control showing local oscillations around discrete steps.

represents the system behavior:

$$\frac{d\varepsilon}{dt} = -K_p\varepsilon = V_a \tag{1}$$

where ε is the position error (mm), K_p is the user-defined proportional control constant (1/s), and V_a is the actuation speed (mm/s) applied by a microcontroller (Texas Instruments MSP430F1612). Three-phase sinusoidal excitation signals are generated by the microcontroller at the actuation frequency:

$$f = \frac{1}{0.36} \left| \frac{d\varepsilon}{dt} \right| \tag{2}$$

As the slider translates, the sequential alignment of through-holes and photodiodes is detected and used to measure position. With a higher resolution than the stepping distance and MHz range operating frequency, the photodiodes have negligible effect on device/control dynamics. A position tracking algorithm has been written using C++ and implemented in the microcontroller. The slider position is calculated by monitoring sequential peaks in three photodiode signals, corresponding to consecutive electrode-pole alignments at a $120 \mu\text{m}$ stepping distance. The direction of motion is determined by observing the order of successive peaks in the discrete photodiode signals. The desired position in Fig. 8, x_d , is input to the microcontroller and compared to the measured position, x_m , obtained from the position tracker, resulting in the position error, $\varepsilon = x_d - x_m$. The desired actuation speed is then calculated as $V_a = -K_p\varepsilon$. Three-phase sinusoidal waveforms traveling at the actuation speed, V_a , are generated by the microcontroller and applied to the device through a high-voltage amplifier, tending the position error to zero.

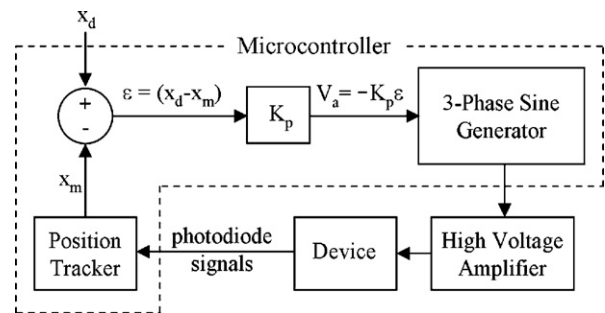


Fig. 8. Block diagram of the control scheme showing various components with proportional control constant (K_p), desired position (x_d), measured position (x_m), position error (ε), and actuation speed (V_a), where the three-phase sine generator and position tracker are sub-programs implemented in the microcontroller.

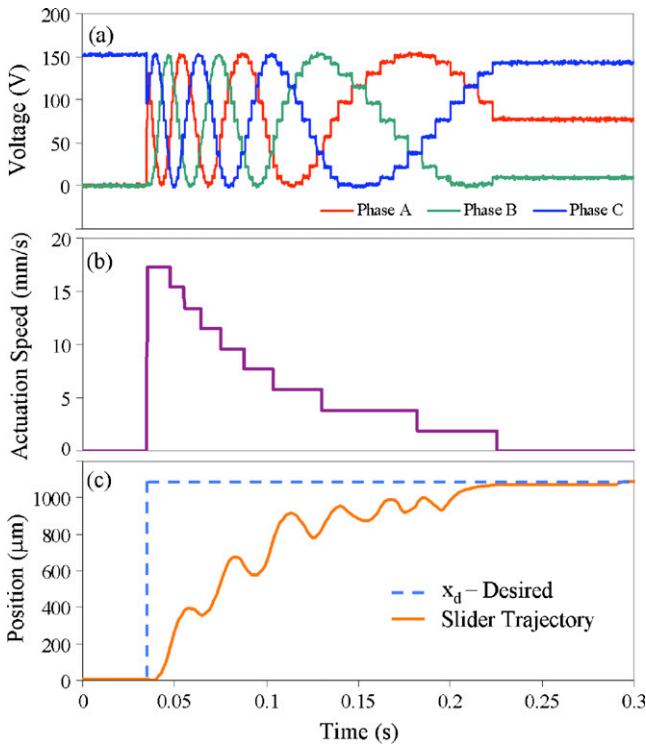


Fig. 9. Control system response to a step in position showing (a) the generated three-phase excitation waves, (b) the corresponding actuation speed, and (c) the desired position and measured slider trajectory.

4.1. Closed-loop step response

In this section, the closed-loop step response of the micropositioner is characterized and the relationship between the settling time and the proportional constant, K_p , is investigated for various stepping distances and actuation voltages. Fig. 9 shows the system response for a $1080\ \mu\text{m}$ step with $K_p = 16$ using the control scheme shown in Fig. 8. For times $0 < t < 0.04\ \text{s}$, the system is in equilibrium with constant voltages applied to the stator resulting in zero actuation speed and equivalent desired and measured positions. At $t = 0.04\ \text{s}$, the input desired position is increased by $1080\ \mu\text{m}$ and the proportional control system responds accordingly. The associated position error drives three-phase sinusoidal excitation signals (Fig. 9a), corresponding to a non-zero actuation speed (Fig. 9b). Fig. 9c shows both the desired position and the slider trajectory tracked by the high-speed camera. As the measured position approaches the desired value, the excitation frequency and resultant actuation speed decrease and eventually go to zero at the new equilibrium position.

The step response of the micropositioner at several values of K_p is shown in Fig. 10 for a $1080\ \mu\text{m}$ step and a peak voltage of $150\ \text{V}$. Individual slider steps can be seen for small proportional control constants ($K_p = 2$), as well as local oscillations due to electrostatic spring effects. As K_p is increased, the actuation speed increases resulting in smaller settling times. This behavior is observed up to a threshold at which point the slider overshoots the desired position prior to reaching equilibrium ($K_p = 16.7$). A further increase in K_p results in erratic motion and a complete loss of synchronization.

The effect of proportional control constant on settling time, defined as the time it takes to settle within 10% of the desired position, is shown in Figs. 11 and 12. Step response analysis has been performed for a distance of $1080\ \mu\text{m}$ at various peak voltages (Fig. 11) and for a peak voltage of $150\ \text{V}$ at various stepping distances (Fig. 12). Fig. 11 shows comparable behaviors for three peak excitation voltages, where the settling time decreases with K_p

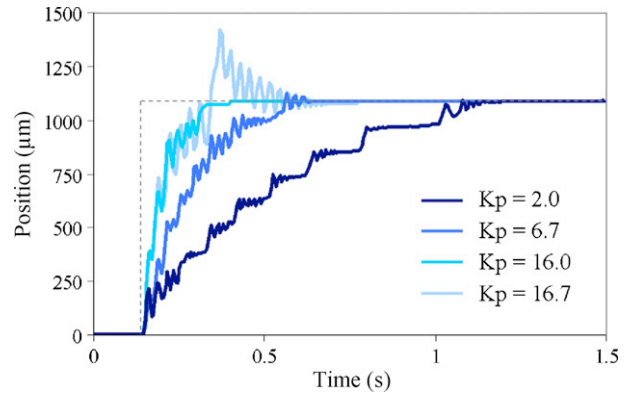


Fig. 10. Micropositioner response for several values of K_p demonstrating variations in settling time for a $1080\ \mu\text{m}$ step.

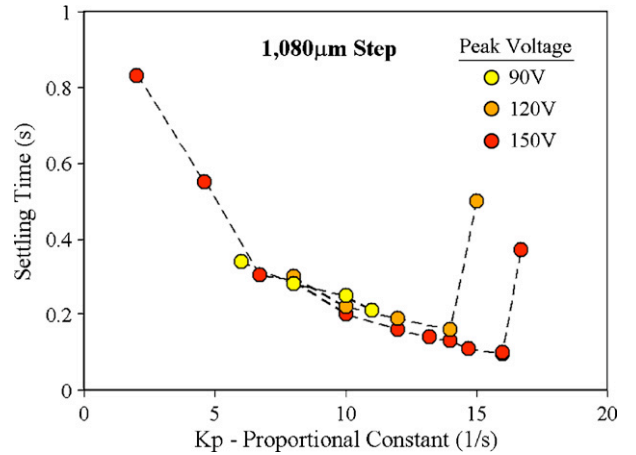


Fig. 11. Micropositioner settling time as a function of proportional control constant for a $1080\ \mu\text{m}$ stepping distance at various actuation voltages.

and then abruptly increases due to overshoot. Each data set terminates at the maximum achievable K_p , above which the device could not maintain synchronization. For higher voltages, stable operation is achieved at larger values of K_p resulting in smaller settling times. Fig. 12 shows similar trends for four stepping distances at a fixed voltage. At large values of K_p , minor discrepancies and erratic behavior can be seen for the smaller distances considered. This is

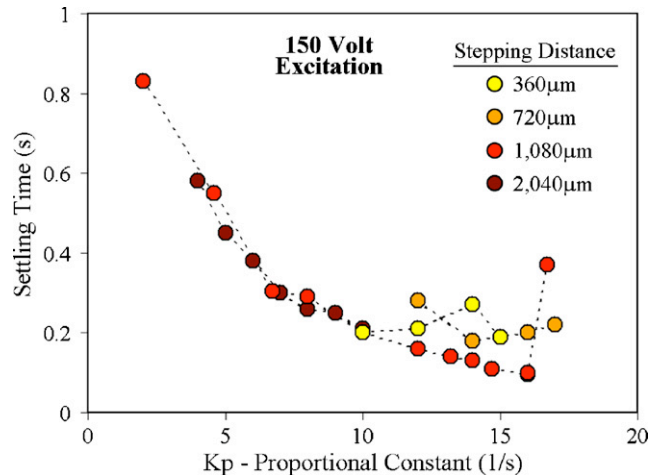


Fig. 12. Micropositioner settling time as a function of proportional control constant at $150\ \text{V}$ peak excitation for various stepping distances.

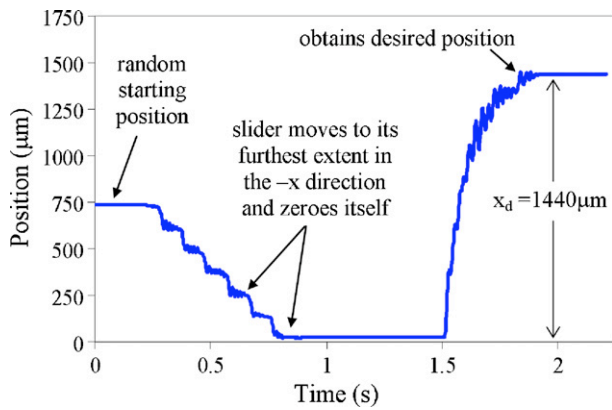


Fig. 13. Demonstration of positioning referenced to a device-defined origin with $x_d = 1440 \mu\text{m}$, $K_p = 10$ at 150 V peak excitation.

attributed to the nature of rolling friction for small steps. For pure rolling motion, a $360 \mu\text{m}$ step corresponds to one-fifth of a full ball rotation. High static friction and a large slide-to-roll ratio are presumed to be dominant factors in this regime.

The step response characterization in Figs. 11 and 12 shows both qualitative and quantitative agreement for excitation voltages above 90 V and stepping distances of up to 2 mm. A minimum settling time of 0.1 s was achieved at 150 V for a $1080 \mu\text{m}$ step. Similarly, a maximum synchronous speed of 20.4 mm/s has been demonstrated, representing a three-fold increase as compared to previously reported designs using open-loop excitation [12].

4.2. Referenced positioning and autonomous response

Implementing this control system, two functions critical for accurate positioning have been achieved; the device can establish a necessary frame of reference and respond autonomously to arbitrary disturbances. Fig. 13 demonstrates referenced positioning. From a random starting position, the slider is moved to the furthest extent of its range and an origin is defined. The slider then steps $1440 \mu\text{m}$ from this device-defined reference. This graph demonstrates the improvement in performance using closed-loop control as compared to Fig. 7. Smooth motion is observed as the slider is actuated twelve minimum stepping distances with a settling time of less than 0.3 s. Fig. 14 shows the device responding to perturbations; the slider returns to the desired position autonomously when forward and backward impulsive forces are applied using a pair of tweezers. These are direct results of closed-loop control, demonstrating the importance of integrated feedback sensors for accurate and reliable micropositioners.

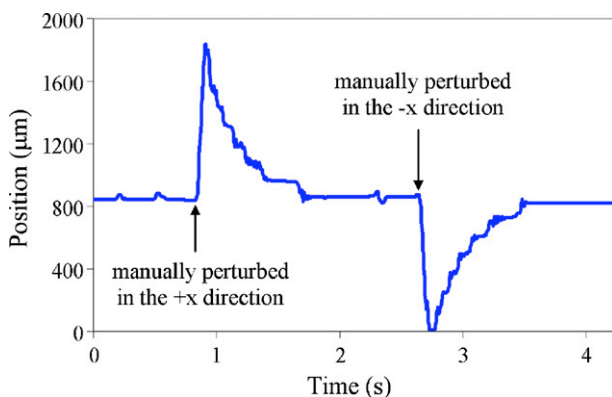


Fig. 14. Demonstration of autonomous response to arbitrary disturbances with $K_p = 3.3$ at 150 V peak excitation.

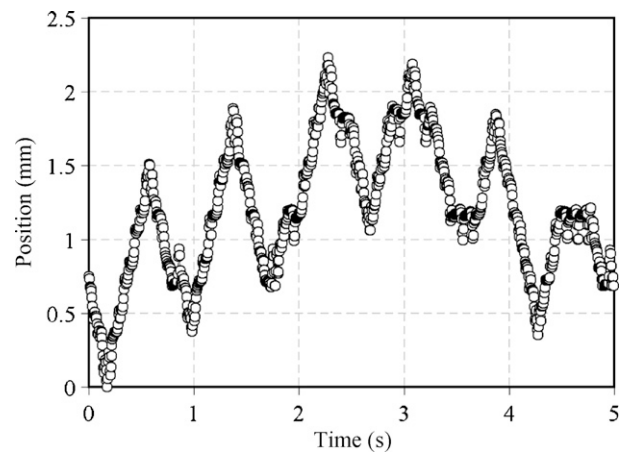


Fig. 15. Continuous operation using open-loop excitation, showing loss of synchronization and erratic behavior.

4.3. Continuous operation

Fig. 15 shows the open-loop response as the slider is continuously excited back and forth using traveling sine waves at 150 V; erratic behavior associated with the loss of synchronization is observed. Implementing closed-loop control, continuous operation of the micropositioner has been achieved without any loss of synchronization under similar loading. Fig. 16 shows the closed-loop trajectory as the slider is actuated to continually toggle between two positions using 150 V excitation, with $K_p = 6.7$. This demonstrates a significant improvement using closed-loop control and the necessity of integrated feedback control for reliable and continuous operation.

4.4. Optimization

While this work demonstrates the feasibility of ball bearing supported micropositioners using integrated feedback control, further optimization is required for high-performance applications. Advanced control architectures using proportional-integral-derivative control and secondary state variables, such as velocity and acceleration, can be implemented to increase speed and accuracy. The use of PID control has not been demonstrated in this work due to noise in the system and the low sampling rate of the microcontroller. Additionally, current research focuses on the integration of solid-film hard coatings such as silicon carbide and ultra-nanocrystalline diamond to reduce bearing friction. The viability of these

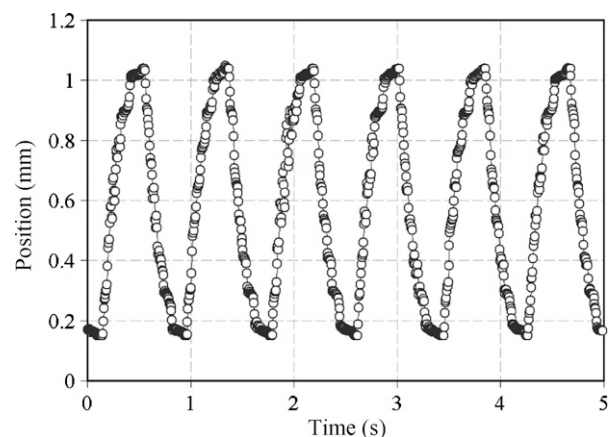


Fig. 16. Demonstration of continuous synchronous operation with $K_p = 6.7$ at 150 V peak excitation.

technologies for application-specific devices requires further investigation into the effects of scale and geometry. In particular, the positioning resolution will be dictated by a combination of the minimum achievable electrode width and ball diameter, while the range is determined by the overall length of the microball housings. Future work will focus on optimizing the drive, support, and sensing mechanisms for application-defined positioning resolution, range, accuracy, and speed.

5. Conclusions

A closed-loop position control system using a photodiode-based position sensing mechanism is implemented in an existing micro-motor design for millimeter-scale micropositioning applications. Using a microball bearing support mechanism and a variable-capacitance drive mechanism, micropositioners with a range of 4 mm and a resolution of 120 μm have been fabricated and characterized. A proportional control law has been implemented and the effect of the proportionality constant has been investigated for various stepping distances and actuation voltages. A minimum settling time of 0.1 s was achieved for a 1 mm step at 150 V. Closed-loop excitation has enabled sustained synchronous motion and a maximum speed of 20.4 mm/s, representing a threefold increase as compared to open-loop operation. Implementing this control system, the micropositioner can establish a necessary frame of reference for accurate positioning and respond autonomously to external disturbances. These functions are a direct result of the use of feedback sensors and could not otherwise be achieved. The closed-loop position control system presented in this work demonstrates the feasibility and functionality of smart microsystems using integrated feedback sensors.

Acknowledgements

This work was supported by the Army Research Office under Grant No. ARMY-W911NF0410176, and Army Research Laboratory under Grant No. CA#W911NF-05-2-0026. The authors would like to thank the U.S. Army Research Laboratory and Maryland Nanocenter personnel for their support in the fabrication of the devices as well as Mr. Konstantinos Gerasopoulos for his contributions to this work.

References

- [1] M. Patrascu, S. Stramigioli, Stick-slip actuation of electrostatic stepper micropositioners for data storage – the μ walker, in: Proceedings of International Conference on MEMS, NANO and Smart Systems, Los Alamitos, CA, USA, 2005, pp. 81–86.
- [2] C.S.B. Lee, S. Han, N.C. MacDonald, Single crystal silicon (scs) xy-stage fabricated by DRIE and IR alignment, in: Proceedings of IEEE 13th Annual International Conference on Micro Electro Mechanical Systems, Miyazaki, Japan, 2000, pp. 28–33.
- [3] I. Shubin, P. LiKamWa, A guided-wave optical switch controlled by a micro-electro-mechanical cantilever, in: IEEE Lasers and Electro-Optics Society 2000 Annual Meeting, vol. 1, Rio Grande, Puerto Rico, 2000, pp. 50–51.
- [4] R.R.A. Syms, Long-travel electrothermally driven resonant cantilever microactuators, *J. Micromech. Microeng.* 12 (2002) 211–218.
- [5] H. Guckel, J. Klein, T. Christenson, K. Skrobis, M. Laudon, E.G. Lovell, Thermomagnetic metal flexure actuators, in: IEEE Solid-State Sensor and Actuator Workshop, Hilton Head Island, SC, USA, 1992, pp. 73–75.
- [6] S.C. Shen, C.T. Pan, H.P. Chou, Electromagnetic optical switch for optical network communication, *J. Magn. Mater.* 239 (2002) 610–613.
- [7] Y. Soeno, S. Ichikawa, T. Tsuna, Y. Sato, I. Sato, Piezoelectric piggy-back microactuator for hard disk drive, *IEEE Trans. Magn.* 35 (1999) 983–987.
- [8] P. Cusin, T. Sawai, S. Konishi, Compact and precise positioner based on the inchworm principle, *J. Micromech. Microeng.* 10 (2000) 516–521.
- [9] L.L. Chu, Y.B. Gianchandani, A micromachined 2D positioner with electrothermal actuation and sub-nanometer capacitive sensing, *J. Micromech. Microeng.* 13 (2003) 279–285.
- [10] D.A. Horsley, N. Wongkomet, R. Horowitz, A.P. Pisano, Precision positioning using a microfabricated electrostatic actuator, *IEEE Trans. Magn.* 35 (1999) 993–999.
- [11] A. Modafe, N. Ghalichechian, A. Frey, J.H. Lang, R. Ghodssi, Microball-bearing-supported electrostatic micromachines with polymer dielectric films for

- electromechanical power conversion, *J. Micromech. Microeng.* 16 (2006) S182–S190.
- [12] N. Ghalichechian, A. Modafe, J.H. Lang, R. Ghodssi, Dynamic characterization of a linear electrostatic micromotor supported on microball bearings, *Sens. Actuators A: Phys.* 136 (2007) 416–503.
- [13] N. Ghalichechian, A. Modafe, R. Ghodssi, P. Lazzeri, R. Micheli, M. Anderle, Integration of benzocyclobutene polymers and silicon micromachined structures using anisotropic wet etching, *J. Vac. Sci. Technol. B* 22 (2004) 2439–2447.
- [14] A. Modafe, N. Ghalichechian, B. Kleber, R. Ghodssi, Electrical characterization of benzocyclobutene polymers for electric micromachines, *IEEE Trans. Device Mater. Reliab.* 4 (2004) 495–508.
- [15] A. Modafe, N. Ghalichechian, M. Powers, M. Khbeis, R. Ghodssi, Embedded benzocyclobutene in silicon (EBiS): an integrated fabrication process for electrical and thermal isolation in MEMS, *Microelectron. Eng.* 82 (2005) 154.
- [16] T.-W. Lin, A. Modafe, B. Shapiro, R. Ghodssi, Characterization of dynamic friction in MEMS-based micro-ball bearings, *IEEE Trans. Instrum. Meas.* 53 (2004) 839–846.
- [17] X. Tan, A. Modafe, R. Ghodssi, Measurement and modeling of dynamic rolling friction in linear microball bearings, *J. Dyn. Syst. Meas. Contr.* 128 (2006) 891–898.
- [18] M. McCarthy, B. Hanrahan, C. Zorman, R. Ghodssi, Rolling friction in MEMS ball bearings: the effects of loading and solid film lubrication, in: STLE/ASME International Joint Tribology Conference, San Diego, CA, USA, October 22–24, 2007.
- [19] N. Ghalichechian, M. McCarthy, M.I. Beyaz, R. Ghodssi, Measurement and modeling of friction in linear and rotary micromotors supported on microball bearings, in: Proceedings of the 21st IEEE International Conference on Micro Electro Mechanical Systems, Tucson, AZ, USA, January 13–17, 2008, pp. 507–510.
- [20] M.I. Beyaz, N. Ghalichechian, R. Ghodssi, Toward an autonomous electrostatic micromotor: integrated feedback control, in: Proceedings of the 21st IEEE International Conference on Micro Electro Mechanical Systems, Tucson, AZ, USA, January 13–17, 2008, pp. 483–486.
- [21] M.I. Beyaz, N. Ghalichechian, R. Ghodssi, Toward smart micromachines with integrated feedback control, in: Presented at International Semiconductor Device Research Symposium, College Park, MD, USA, 2007.
- [22] M.I. Beyaz, N. Ghalichechian, R. Ghodssi, Towards feedback control with integrated position sensing in micromachines, in: Presented at AVS International Symposium and Exhibition, Seattle, WA, USA, 2007.

Biographies

Mustafa Ilker Beyaz received the B.S. degree in electrical and electronics engineering from the Middle East Technical University, Ankara, Turkey, in 2005 and the M.S. degree in electrical engineering from the University of Maryland, College Park, MD, in 2008. His research interests are in the design and development of power MEMS devices with various actuation mechanisms for small scale energy conversion and micromachine control systems. He is currently working towards his Ph.D. degree in electrical engineering under the guidance of Prof. Reza Ghodssi at the MEMS Sensors and Actuators Laboratory.

Matthew McCarthy received the B.S. degree in aerospace engineering from Syracuse University, Syracuse, NY, in 2002 and the M.S. and Ph.D. degrees in mechanical engineering from Columbia University, New York, NY, in 2004 and 2006, respectively. He was a Postdoctoral Research Associate with the MEMS Sensors and Actuators Laboratory in the Department of Electrical and Computer Engineering at the University of Maryland from 2007 to 2008. He is currently a Postdoctoral Research Associate in the Mechanical Engineering Department at the Massachusetts Institute of Technology. His research interests are in the field of emerging power MEMS and micro-cooling technologies as well as multi-scale thermal-fluid sciences. His current efforts are focused on the development of compact cooling systems, ball-bearing-supported micromachines, tribological characterization of microscale rolling contacts, nanostructured energy storage devices, and sensors and actuators.

Nima Ghalichechian received his Ph.D. in Electrical Engineering from the University of Maryland-College Park in August 2007. For his Ph.D. research he developed the first rotary micromotor supported on microball bearings. His dissertation is titled “Design, Fabrication, and Characterization of a Rotary Variable-Capacitance Micromotor Supported on Microball Bearings”. In 2007 Nima joined the MEMS Research department at FormFactor Inc, Livermore, California developing micro springs for wafer-level probe cards. Nima is recipient of the 2006 American Vacuum Society (AVS) Graduate Research Award and 2007 George Harhalakis Outstanding Systems Engineering Graduate Student Award, Institute for Systems Research (ISR), University of Maryland. Nima is a member of IEEE and Sigma Xi.

Reza Ghodssi is the Herbert Rabin Distinguished Associate Professor and Director of the MEMS Sensors and Actuators Lab (MSAL) in the Department of Electrical and Computer Engineering (ECE) and the Institute for Systems Research (ISR) at the University of Maryland (UMD). He is also affiliated with the Fischell Department of Bioengineering (BIOE), the Maryland NanoCenter, the University of Maryland Energy Research Center (UMERC), and the Materials Science and Engineering Department (MSE) at UMD. Dr. Ghodssi's research interests are in the design and development

of microfabrication technologies and their applications to micro/nano devices and systems for chemical and biological sensing, small-scale energy conversion and harvesting. Dr. Ghodssi has over 62 scholarly publications, is the co-editor of the "Handbook of MEMS Materials and Processes" to be published in 2009, and is an associate editor for the Journal of Microelectromechanical Systems (JMEMS) and

Biomedical Microdevices (BMMD). Dr. Ghodssi has received the 2001 UMD George Corcoran Award, the 2002 National Science Foundation CAREER Award, and the 2003 UMD Outstanding Systems Engineering Faculty Award. Dr. Ghodssi is the co-founder of MEMS Alliance in the greater Washington area and a member of the IEEE, AVS, MRS, ASEE and AAAS societies.